ENCIT 2018

ABCM Associação Brasileira de Engenharia e Ciências Mecânicas

17th Brazilian Congress of Thermal Sciences and Engineering
November 25th-28th, 2018, Águas de Lindóia, SP, Brazil

ENCIT-2018-0788
DEVELOPMENT OF A DYNAMIC MASKING PROCEDURE FOR THE TAYLOR BUBBLE IDENTIFICATION IN THE PIV/LIF TECNHIQUE APPLICATION FOR SLUG FLOW

R.F.L. Cerqueira, rafaelfc@sinmec.ufsc.br[1]
E.E. Paladino, paladino@sinmec.ufsc.br[1]
B.K. Ynumaru, ynumaru@gmail.com[1]
C.R. Maliska, maliska@sinmec.ufsc.br[1]

SINMEC - Computational Fluid Dynamics Lab Mechanical Engineering Department, Federal University of Santa Catarina, 88040-900 - Florianopolis - SC - Brazil
rafaelfc@sinmec.ufsc.br, paladino@sinmec.ufsc.br, ynumaru@gmail.com, maliska@sinmec.ufsc.br

Abstract. *This work presents a technique for the generation of dynamic masks for the measurement of velocity fields around Taylor bubbles by the PIV/LIF technique. The characterization of the flow around a Taylor bubble is important for the understanding of the physical phenomena associated with slug flow patterns. For the acquisition of averaged liquid velocity fields, it is necessary to remove the Taylor bubble from the images acquired by the PIV/LIF technique. The usual practice for this task is the application of a static mask that does not take into account the deformation of the Taylor bubble. However, none of the techniques found in the literature is able to deal with flows with dispersed bubbles and high inverse viscosity numbers which presents great fluctuations in the velocity field and also in the shape of the Taylor bubble. Thus, the present work aims to develop a method for the generation of dynamic masks for the removal of Taylor bubbles in the PIV/LIF technique in flows with dispersed bubbles and high inverse viscosity number. By comparing the average liquid velocity fields around the Taylor bubbles in flows, it is observed that the interaction between the dispersed and Taylor bubbles modify the flow structure around the Taylor bubbles and its shape.*

Keywords: *Particle Tracking Velocimetry, PIV, Taylor bubble, slug flow, dynamic masking*

1. INTRODUCTION

The measurement of flow variables in two-phase gas-liquid flows has been a challenging task for scientists and engineers over decades. The highly transient behavior and strong spatial variations of these flows lead to the need of some kind of averaging in order to get consistent values of the measured variables, which can be used for models closure and/or validation. Generally, local or instantaneous measurements cannot give a meaningful representation of the flow behavior in two-phase flows.

Among the flow patterns encountered for gas-liquid flows in ducts, the slug pattern has drawn special attention of researchers mainly because of its intermittent characteristic which, in oil production systems, can be associated to difficulties in control system operations due to the strong pressure and velocity fluctuations and system damage in the case of sever slug conditions. Additionally, this intermittent characteristic brings additional difficulties in measuring flow variables for this flow pattern.

Thus, in order to get a deeper insight of this flow pattern, several researchers presented experimental studies and techniques aiming the detailed measurement of the flow fields around Taylor bubbles, most of them using Particle Image Velocimetry techniques - PIV (Bugg and Saad, 2002; Van Hout *et al.*, 2002; Nogueira *et al.*, 2003; Sousa *et al.*, 2005; Nogueira *et al.*, 2006; Sousa *et al.*, 2006b,a; Santos and Coelho Pinheiro, 2014). Nevertheless, these works consider a very simplified figure of the flow around Taylor bubbles, particularly, when compared with the flow of these bubbles in real slug flow. The main aspect, to the knowledge of the authors, which has not been hitherto taken into account in previous experimental research works, is related to the presence of small dispersed bubbles in the liquid stream. In real applications, Taylor flow is usually encountered in mini and microchannels, or in cases of very low superficial liquid velocities, which promotes the coalescence of small bubbles. In addition, most of these previous studies usually consider very low values of the inverse viscosity number which is defined as, $N_f = \sqrt{\rho^2 g D^3/\mu^2}$ and represents a relation between gravitational and viscous forces. Recalling that gravity is the driving force for the Taylor bubbles displacement, relative to the liquid

stream, this number can be also related to the bubble Reynolds number ($Re = \rho_L U_{tb} D/\mu_L$), based on its velocity (in fact, $N_f = \rho_L U_{tb} D/\mu_L \times \sqrt{gD}/U_{tb} = Re/Fr$) and thus, is it related to the fluctuating behavior of the liquid phase flow. When N_f is set to low values, flow is stable, and thus, instantaneous velocity fields or averages of a low number of instantaneous fields can give a consistent representation of the flow behavior around Taylor bubbles. On the other hand, large values of the inverse viscosity number, which are common in real slug flows, lead to strongly fluctuating flow, mainly in the wake region of the Taylor bubbles. The presence of dispersed bubbles in the liquid stream increases these fluctuations. In these cases, a large number of instantaneous fields is necessary to get a consistently averaged flow field around Taylor bubbles.

Van Hout *et al.* (2002) used the PIV technique to study the induced flow by the passage of Taylor bubbles in stagnant water, in a 25 mm ID duct (N_f = 12300), reporting the use of about 100 instantaneous fields for the calculation of the averaged fields. On this work, despite the shod results of the averaged velocity field around the Taylor bubbles nose and wake region, there is no discussion about the masking procedure, in which the Taylor bubble is removed from the PIV analysis.

Nogueira *et al.* (2003, 2006), using the PIV technique and, presented results of the flow around Taylor bubbles in stagnant and co-current liquid flow for N_f ranging from 17 to about 18,000. They reported the use of 7 to 20 instantaneous fields for the calculation of averaged fields. Nevertheless, even for relatively low values of $N_f \approx 800$, visual observation of the vector fields and streamlines show the presence of several fluctuations, indicating that those fields are far from being representative of the averaged ones. To remove the Taylor bubbles from the PIV velocity fields, the authors use the Pulsed Shadowgraphy Technique (PST), which produces "binary masks" from the perpendicular projection of the Taylor bubbles into the camera plane.

The present work shows a detailed description of the experimental apparatus used to generate the flow of Taylor bubbles with controlled sizes in a bubbly flow stream, and of the instrumentation specifically developed to measure the velocity field around Taylor bubbles using the PIV technique, in repeatable conditions such that it allows for the calculation of consistently averaged fields in several flow conditions. In order to remove the Taylor bubbles from the PIV images, a dynamic masking procedure was developed to remove the Taylor bubbles from the PIV images, since the PST technique described in (Nogueira *et al.*, 2003, 2006) is not suitable on the presence of dispersed bubbles due to the superposition of bubbles shadows on the camera plane.

2. METHODOLOGY

2.1 Experimental setup

This section describes the experimental apparatus that was specially designed for this research. This system allows for the generation of a single phase liquid stream or bubbly flow in a straight vertical duct where Taylor bubbles, with controlled size, are injected. Thus, the superficial velocities of liquid and dispersed bubbles phase can be independently controlled, as well as the size and frequency of the Taylor bubbles, which are independently injected into the stream. These controlled conditions are necessary since, maintaining the sizes, and so velocities of Taylor bubbles, the velocity fields around the different bubbles are expected to be similar except for fluctuations.

The experimental apparatus is schematically depicted in Fig. 1a). The test section consists of a transparent pipe with $D = 26.2$ mm internal diameter and $L = 2.0$ m length.

At the PIV measurement section, a box constructed with transparent acrylic, made with 8 plane faces, filled with the water is included to minimize optical distortion. A two-phase stream is generated at the bottom of the test section by combining a liquid stream (tap water), driven by a centrifugal pump, and air from the compressed air line from the building. The dispersed bubbles are injected at the bottom of the tube, and the gas superficial velocity is measured by two OMEGA FL-3802ST/FL-3861SA flow meters with ranges of 81.4-814.0 standard mL/min and 26.3-263.0 standard mL/min, both with $\pm 2.0\,\%$ full scale accuracy. The flow rate is controlled by a needle valve downstream. In order to correct the gas superficial velocity due to gas expansion, a pressure and a temperature sensors were installed downstream the needle valves. Therefore, the measured gas superficial velocities (for dispersed bubbles) were corrected to take into account the gas expansion. As the return to the reservoir consists of a relatively short (~ 0.5 m), and 50.0 mm internal diameter duct, and the reservoir is opened to the atmosphere, it was assumed that the pressure at the test section was close to the atmospheric pressure. A porous gas diffuser was installed in the bottom of the tube, in order to control the sizes of the dispersed bubbles.

The water flow rate is measured by an OMEGA FL46303 flow meter with a range of 1.00-7.50 l/min with $\pm 5.0\,\%$ full-scale accuracy. The liquid flow rate is controlled by a frequency inverter connected to the electric water pump motor.

The Taylor bubbles are injected through a lateral connection "Y" at the bottom of the column. The injection system is formed by a reservoir with a known volume, which has at its two ends an electronically actuated solenoid valves. From the pressure of the compressed air line, it is possible to control the volume of the Taylor bubble to be injected, since the reservoir has a constant volume. An electronic system controls the injection cycles of the Taylor bubbles, from the valve opening and closing command.

Initially, the valve 1 opens, filling the reservoir with known volume with compressed air at a given pressure. After a specific time, the valve 1 is closed for equalization of the system pressure and the initially closed valve 2 is actuated,

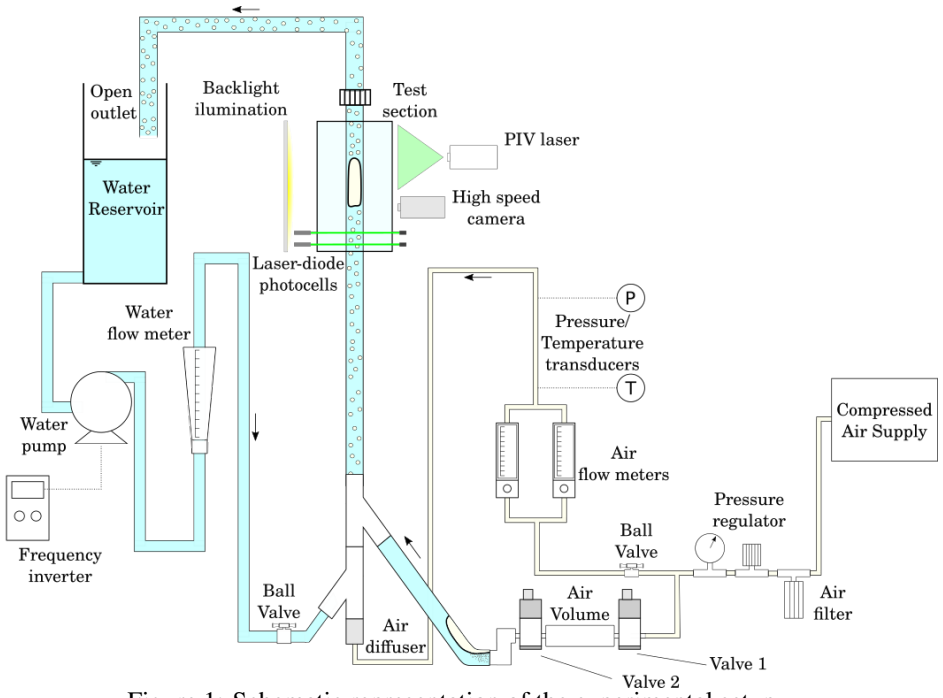

Figure 1: Schematic representation of the experimental setup.

releasing the volume of air that is led by a hose to the liquid filled duct, becoming a bubble of Taylor. ($t_{stab.}$) and the waiting time between the different generation cycles (t_{wait}), were electronically controlled. The Taylor bubble injection system is controlled by an Arduino UNO R3 Atmega328P, which communicates through an USB interface with a dedicated PC application developed in NI LabView software.

2.2 PIV/LIF Technique

The Particle Image Velocimetry (PIV), an optical measurement technique, consists of the addition of tracer particles in the flow, which after being illuminated by a luminous plane, are recorded through an image acquisition and post-processed method to obtain a velocity field. The PIV measurement technique is widely used in the field of fluid mechanics (Raffel *et al.*, 2007), in particular in the validation of numerical results obtained by CFD, since the method is able to provide detailed velocity fields.

In liquid-gas two-phase applications, in the presence of interfaces with a longer length than the tracer particles, the light originating from the light source of the PIV system ends up being scattered by the interfaces. This scattered light has a much higher intensity than that of the particle tracing, obfuscating the presence and the subsequent acquisition of the same, damaging the quality of the velocity fields obtained due to the lower level of correlation. Thus for this sort of flows, the use of the PIV technique in conjunction with the Laser Induced Fluorescence (LIF) technique is recommended. The PIV/LIF technique consists of the use of fluorescent tracer particles that receive light at a given wavelength (light source) and fluoresce at another wavelength, in which only the less intense "fluorescent" light is captured by the camera through the use of optical filters. In this way, the acquisition of light from the light source spread through the gas-liquid interface is avoided, reducing in part the problems regarding the use of the PIV technique in liquid-gas flows.

The test section filled with liquid is used to minimize optical distortions as a function of the different refractive indexes of the liquid and the material of the duct walls. In this arrangement, the walls of the test section and that of the vertical duct have a material transparent to the wavelength of the coherent light source. The light source has an approximate wavelength of λ = 532nm (near the green color), while the particles fluoresce near λ = 590nm (close to the pink color). Thus, by positioning a filter that allows the passage of light with wavelengths greater than $\lambda = 590nm$, only the tracer particles will be acquired by the camera.

Although the LIF technique allows the use of the PIV measurement technique in multiphase flows, it does not solve all the problems related to the presence of interfaces. Figures 2 and 3 show images obtained by a high-resolution camera acquired with the PIV technique in conjunction with the LIF technique in the nose and tail region of different Taylor bubbles.

As seen in Figs. 2 and 3, despite the tracer particles are present only in the liquid phase, they appear inside the Taylor and the dispersed bubbles. These “ghost” particles are reflections of the tracer particles in bubble interfaces. Additionally, some of them are the product of reflections of the light scattered by the dispersed bubbles. Due to this scattering/reflected tracer particles, the PIV cross-correlation algorithm will result in valid vectors in these regions, whose physical meaning is

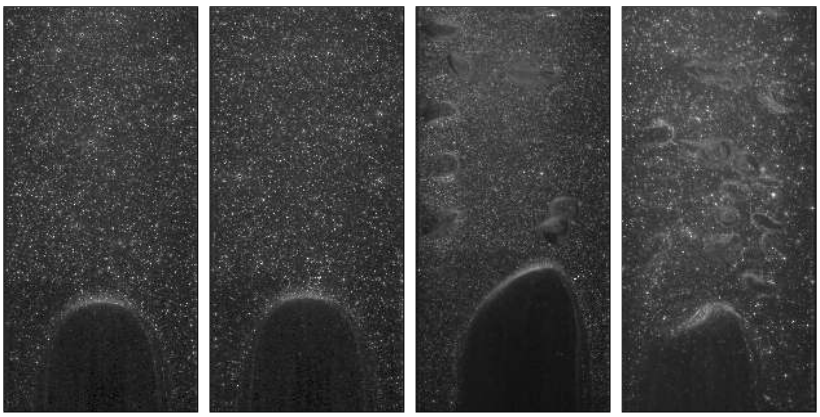

(a) (b) (c) (d)

Figure 2: Images obtained by a high-resolution camera acquired with the PIV/LIF technique in the nose region of different Taylor bubbles: a) e b): Taylor bubble rising in a stagnant fluid column; c) e d): Taylor bubbles rising in a stagnant fluid column with the presence of dispersed bubbles ('*quasi-slug*" flow regime with a gas void fraction value $\alpha_g \approx 10.0\%$.)

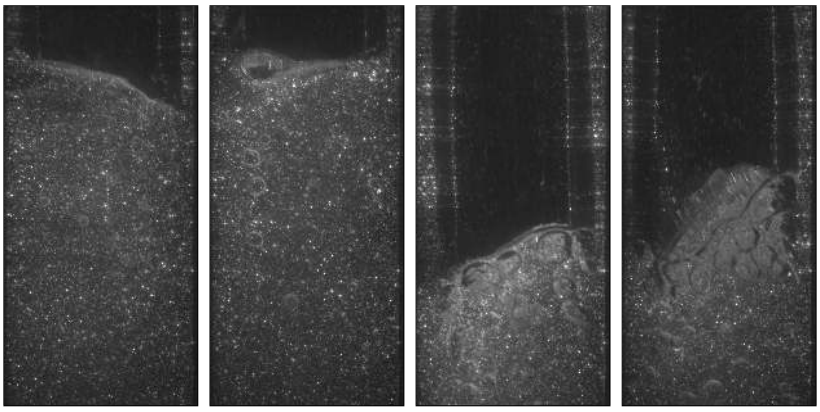

(a) (b) (c) (d)

Figure 3: Images obtained by a high-resolution camera acquired with the PIV/LIF technique in the bottom region of different Taylor bubbles: a) e b): Taylor bubble rising in a stagnant fluid column; c) e d): Taylor bubbles rising in a stagnant fluid column with the presence of dispersed bubbles ('*quasi-slug*" flow regime with a gas void fraction value $\alpha_g \approx 10.0\%$.)

null since the particles are in the liquid phase. In order to solve the problem, it is necessary to implement a mechanism of synchronization between the passage of the bubbles and the moment of the acquisition of the images by PIV (Van Hout *et al.*, 2002; Nogueira *et al.*, 2006, 2003; Meneghini, 2014), thus maintaining the nose and tail of the Taylor bubble always in the same position. However, as seen in Figs. 2 and 3, due to the high number of inverse viscosity N_f, the shape of the tail of the Taylor bubble is not always the same with each acquisition. Besides, in the presence of dispersed bubbles, the nose of the Taylor bubbles is distorted due to the complex interactions between the Taylor bubble and the scattered bubbles in the nose region. Thus, an additional procedure is required for the removal of the tail region and the nose in the images obtained by PIV, making it possible to obtain medium velocity fields of the liquid around the Taylor bubble flowing in a column with and without the presence of scattered bubbles.

3. TAYLOR BUBBLE IDENTIFICATION

As discussed on the previous paragraphs, due to the high inverse viscosity number N_f and the presence of the dispersed bubbles on the flow stream, the laser diode photocell based synchronization system alone is not sufficient to acquire ensemble averaged velocity fields around the Taylor bubbles. Thus, a dynamic masking procedure is necessary to remove the Taylor bubbles from the PIV images.

In the literature, only the works of Nogueira *et al.* (2003) and Nogueira *et al.* (2006) describe a method for generating the masks around the Taylor bubble. However, these methods are based on the Pulsed Shadow Technique (PST) and cannot be used for dispersed bubble flows, since the technique captures bubbles outside the light sheet of the PIV images. Additionally, these works do not present velocity averaged fields around Taylor bubbles, showing only instantaneous velocity fields. On the work Van Hout *et al.* (2002), the author analyzes the flow around Taylor bubbles rising in stagnant

water columns through velocity averaged fields. However, there is no discussion about the methodology used to mask the Taylor bubbles out of each instantaneous frame and therefore computed the ensemble averaged velocity fields.

This section describes the dynamic masking procedure used in this work to remove the Taylor bubbles nose and bottoms from the original PIV images, detailing the image processing steps for these two regions.

The authors developed the dynamic masking procedure algorithms described in this section through the OpenCV Bradski (2000) library.

3.1 Taylor bubble nose

As shown in Figs. 2 and 3, in the "quasi-slug" flow experiments, the PIV synchronization only ensures that the frame will focus on a selected region (nose or wake), not the bubble position. In order to extract velocity information from these PIV frames and to remove the Taylor bubble nose, a dynamic masking procedure is performed.

Figures 4a and 4b shows the image and signal processing steps to create the dynamic masks, that are going to be detailed on the next paragraphs.

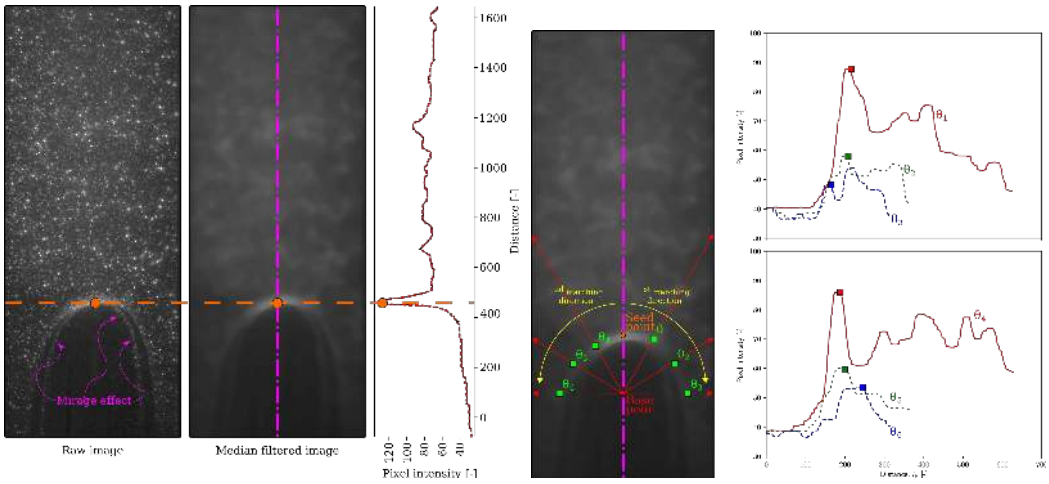

(a) (b)

Figure 4: a) Image filtering operations and the pixel intensity sampling at the duct centerline used to find the Taylor bubble nose "seed point" used for the complete gas-liquid interface procedure. b) Example of the pixel intensity profiles radially sampled from the median filtered image, which shows the Taylor bubble "seed point" and the base point used to sample the image in a radial fashion.

On the first step, the original raw image passes through a median filter. Since the nose shape alters from frame to frame, especially on the case with dispersed bubbles, it is necessary to find a "seed point" from which the nose shape can be reconstructed. In all the acquired nose region PIV frames from this work, a very distinct pattern emerges from the median filtered image. This pattern is characterized by an area with brighter pixel intensity compared to the rest of the image, located near the duct centerline. Then, the first operation is to find the "seed point" from this bright distinct pattern, by analyzing the pixel intensity in the duct centerline. The pixel intensity is shown in Fig. 4a and it can be seen that the first local intensity maximum value represents the gas-liquid interface on this position. In order to find this point, the 8-bit unsigned integer values of the pixel intensity are transformed to float type, so a 1D moving average operation is used to smooth out this signal. In Fig. 4a, the smoothed signal is indicated by the red dotted line. The local maximum is found from these smoothed signals and is represented by the orange plots on the pixel intensity plots in Fig. 4a.

After this "seed point" is found, a gas-liquid interface search is performed radially, through the same pixel analysis sampling mentioned in the paragraph above. Thus, a base point is defined, from where the radial pixel intensity profiles are going to be extracted. The local minimum search operation is carried by these radially extracted intensity profiles. Figure 4b shows this operation, where the sampling is performed from a θ interval of $[0.0, \pi/2]$. This interval can be modified according to the image intensity of the raw PIV acquisition. The base point is positioned at a predefined distance from the seed point since the PIV images are not always captured in the same position for each frame.

As depicted in Fig. 4b, this radial search operation is performed direction-wise, for the reasons described below. After the seed point is found, an additional verification is performed to avoid spurious gas-liquid interface points. This additional procedure compares the distance between the possible gas-liquid interface position between two successive θ marching steps. Then, since the points located on duct centerline have a higher probability to be located in the gas-liquid interface region, if a small marching θ angle is used on the searching procedure, the nearest point from the $(i-1)$th step resulted point is likely to be actual gas-liquid interface position. Since the centerline points are always correctly identified and the interface reconstruction is performed in a marching fashion, in the case of multiple local maxima, the actual gas-liquid

interface position is more likely to be identified. Additionally, this step avoids the location of spurious points, introduced by the fluorescent tracer particles near the gas-liquid interface, as discussed by Nogueira *et al.* (2003), which mirages the interface, as seen in Fig. 4a. It is important to state that the median filter operation, shown in Fig .4a, removes most part these false gas-liquid interface positions through its filtering, reason why the median filter averaged image is used on the procedures described above.

Figure 5 shows the obtained mask for three flow configurations, where the red filled PIV interrogation windows represents the velocity vector removed due to the Taylor bubble nose presence on the frame. This illustration shows that the spurious velocity vectors from the Taylor bubble is completed removed from the PIV frame for three distinct flow configurations. Additionally, Fig. 5 shows a cyan filled interrogation window, which is the Talor bubble nose tip position, acquired during the gas-liquid interface reconstruction procedure. This position, defined as the gas-liquid interface extreme point, is used as the reference position in the averaging process.

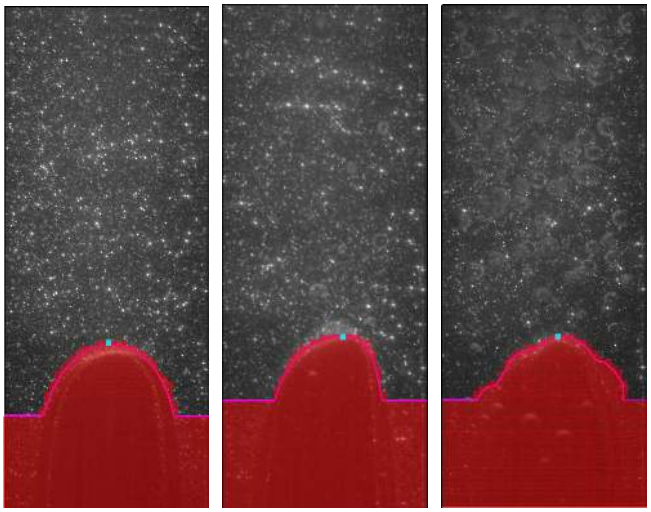

(a) (b) (c)

Figure 5: Masking procedure applied in the PIV frames, where the red filled region represents the discarded velocity vectors. The final mask is shown for three flow stream configurations: a) without the presence of dispersed bubbles; b) with dispersed bubbles injected into the flow stream ($\overline{\langle \alpha_g \rangle} = 1.30\%$); c) with dispersed bubbles injected into the flow stream ($\overline{\langle \alpha_g \rangle} = 4.90\%$).

3.2 Taylor bubble bottom

As for the dynamic masking procedure used in the Taylor bubble nose PIV frames, the first step adopted for the bubble bottom position is the identification of a specific pattern that could be used as an initial "seed point" in the duct centerline. Figure 6 schematically illustrates this image analysis step. Again, the raw PIV image frame is passed through a median filter, which returns a "blurred" image with brighter (strong pixel intensity) in the duct centerline. Thus, the local maxima position of these pixel intensity values encountered in the duct centerline is used as a "seed point" for the gas-liquid interface reconstruction.

After the seed point is found, it is necessary to perform a local analysis operation to found the gas-liquid interface points. Thus, reconstructing the Taylor bubble bottom interface, allowing the removal of the unwanted PIV velocity vectors located inside this region. As seen in Fig. 6, as for the Taylor bubble nose dynamic masking procedure, the application of a median filter alleviates the mirage effect near the gas-liquid interface. For this reason, the median filtered image is used on the local analysis procedure, since this approach avoids the capture of spurious gas-liquid interface points related to the mirage effect. Due to the Taylor bubble bottom shape, there is no need to perform a radial search procedure – as the one used for the Taylor bubble nose dynamic masking procedure – since the gas-liquid interface presents a simpler geometry as those found in the Taylor bubble nose PIV frames. Hence, a simpler line search along the "x" position is performed. However, the line search analysis is still carried out in a marching fashion, using the same nearest-point neighbor condition described in the previous subsection.

Figure 7 illustrates the mask used to remove the Taylor bubble bottom region for three different flow stream configurations. As described in the paragraphs above, the obtained mask is not used to erase the pixel information of the original PIV frame, but to discard the information of the interrogations windows that lie inside this region. This means that the dynamic masking procedure is performed after the computation of the velocity field by the PIV cross-correlation procedure.

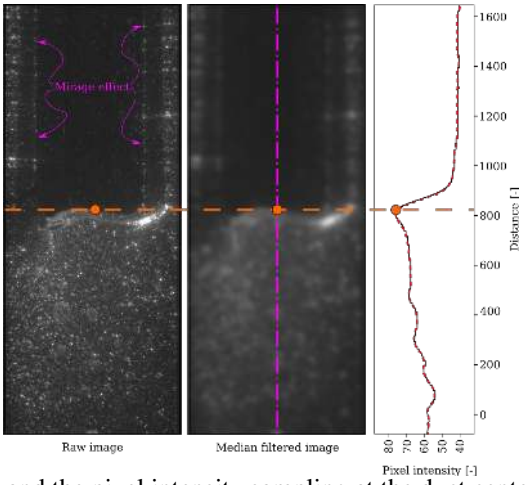

Figure 6: Image filtering operations and the pixel intensity sampling at the duct centerline used to find the Taylor bubble bottom "seed point" used for the gas-liquid interface reconstruction procedure.

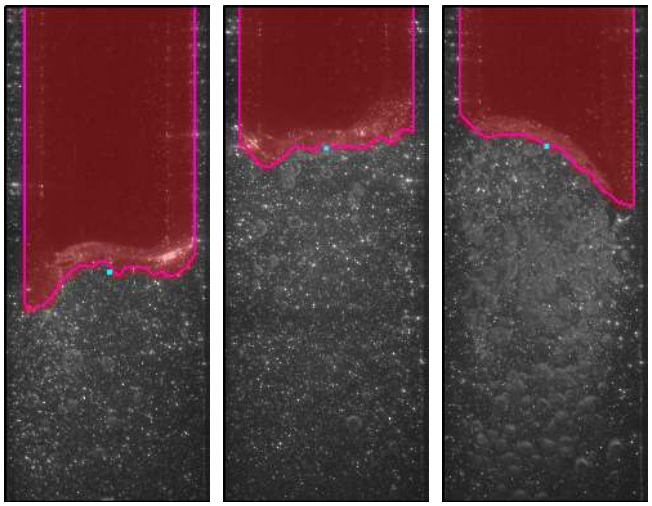

(a) (b) (c)

Figure 7: Masking procedure applied in the PIV frames, where the red filled region represents the discarded velocity vectors. The final mask is shown for three flow stream configurations: a) without the presence of dispersed bubbles; b) with dispersed bubbles injected into the flow stream ($\overline{\langle \alpha_g \rangle} = 1.30\%$); c) with dispersed bubbles injected into the flow stream ($\overline{\langle \alpha_g \rangle} = 4.90\%$).

4. RESULTS

4.1 PIV velocity fields around Taylor Bubbles

After the dynamic masking application and the subsequential change of reference, the method described in Cerqueira *et al.* (2018) is used to remove the dispersed gas phase contribution from the PIV liquid velocity vector. Figure 8 shows the instantaneous liquid velocity vector field around Taylor bubbles, where the dispersed bubbles are present on the flow.

As seen in Fig. 8, the method presented in this work removes correctly identify and remove the Taylor bubbles from the raw PIV image. Hence, it is possible to compute consistent ensemble averaged liquid velocity fields from instantaneous fields like the ones shown in Fig. 8.

Figure 9 presents the ensemble average liquid velocity vector fields near the nose and tail region. In Fig. 9 the thick red line in the vector fields indicates the gas-liquid interface acquired from the PIV dynamic masking procedure. In both cases (nose and bottom), this line is defined as the 0.5 isoline value of the PIV Taylor bubble nose/tail probability occurrence, computed from the PIV results. Additionally, it is interesting to note that in Fig. 9 the PIV dynamic masking procedure is capable to capture the typical curvature of the Taylor bottom shape.

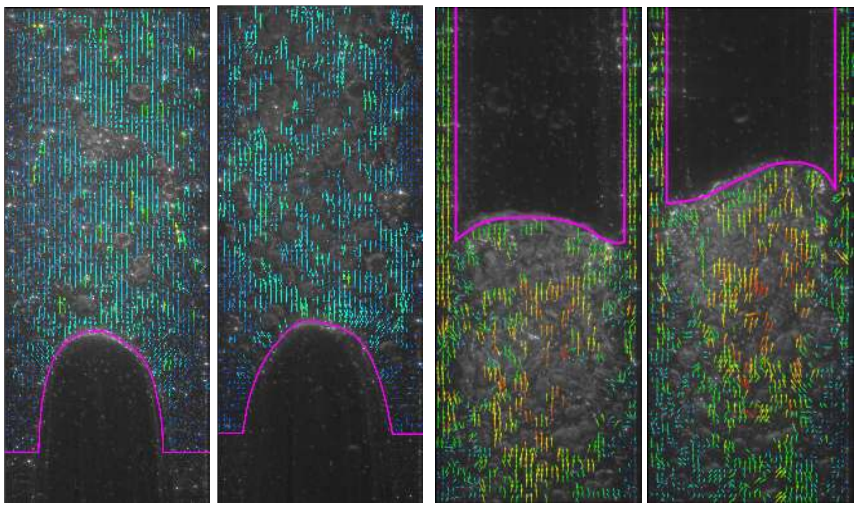

(a) (b)

Figure 8: Example of the instantaneous liquid velocity vector field around Taylor bubble noses (a)) and bottom (b)), where the dispersed bubbles are present on the flow. The interrogations windows where the dispersed bubbles are present are removed by the phase-discrimination method described in Cerqueira *et al.* (2018).

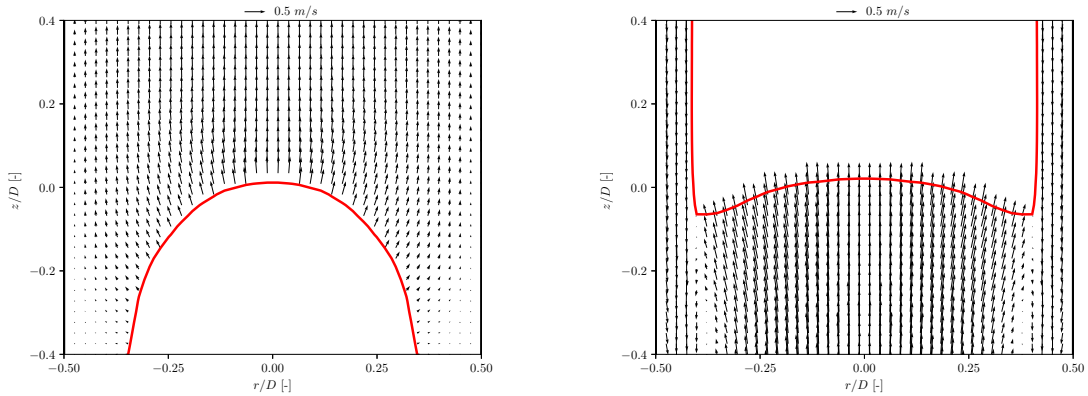

(a) (b)

Figure 9: Ensemble average liquid velocity vector fields around a Taylor bubble for a j_l = 21.64 $\times 10^{-2}$ m/s, j_g = 19.83 $\times 10^{-3}$ m/s and α_g = 4.9 $\%$ flow stream configuration ("quasi-slug" flow). The liquid velocity fields were extracted from an ensemble average over 400 instantaneous fields.

4.2 Velocity fields around Taylor bubbles in co-current flow in the presence of small dispersed bubbles

Figure 10 presents typical velocity profiles at the nose and wake region for different values of small dispersed bubble in the liquid stream. It is important to point out that this superficial velocity of the gas phase corresponds only to the dispersed bubbles, which is calculated from the gas flow rate measured at the gas flowmeter, as the Taylor bubbles air injected independently in the bubbly flow generated at the test section. The value of the volume fraction of dispersed bubbles, shown in the figures, was estimated from the superficial velocity, as described in Cerqueira *et al.* (2018).

Figure 11 shows the streamlines at the wake region of Taylor bubbles for different concentration of gas dispersed bubbles in the liquid stream. The results of Fig. 11 are shown from a reference frame moving with the Taylor bubble, .i.e., the average liquid velocity is subtracted by Taylor the bubble nose velocity. Clearly, even in a low concentration, the presence of dispersed bubbles in the liquid stream significantly affects the flow structure around Taylor bubbles. One of the most evident aspects is the decrease of the recirculation length at the wake region of Taylor bubbles. The length of this recirculation can be directly associated to the bubble terminal velocity and also to the heat and mass transfer coefficients in the liquid slug region.

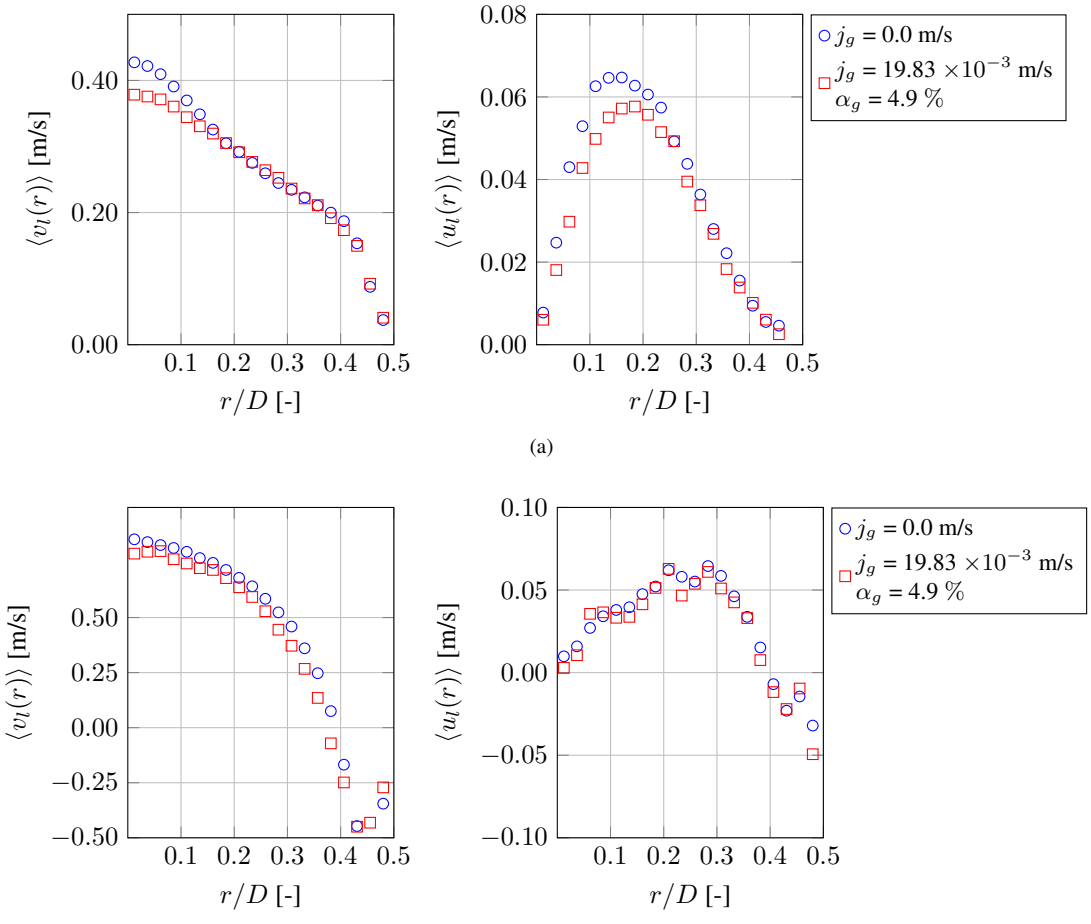

Figure 10: Velocity profiles at the tail and nose regions, for different gas superficial velocities of the dispersed bubble with the same liquid superficial velocity j_l = 21.64 $\times 10^{-2}$ m/s. The plots on the left were taken in the $z/D = 0.06$ position from the bubble nose position. The plots on the right were taken in the $z/D = -0.4$ position from the bubble tail position. The liquid velocity fields were extracted from an ensemble average over 400 instantaneous fields.

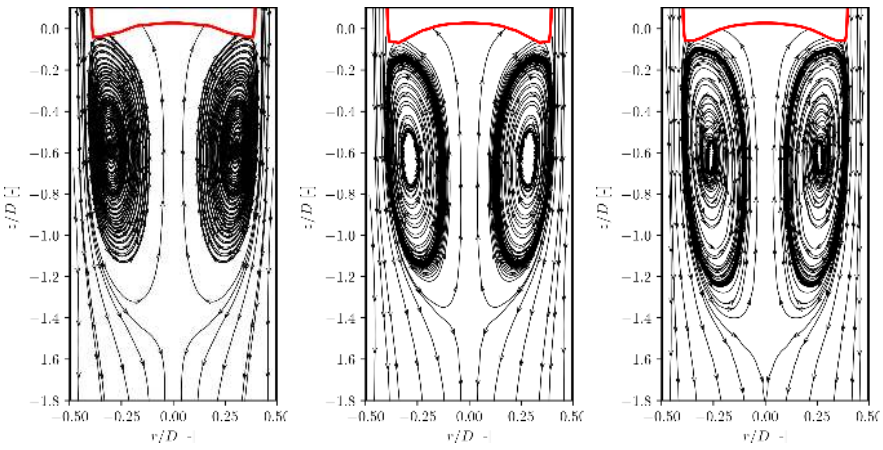

Figure 11: Streamlines at the wake region of Taylor bubbles, for different concentration of dispersed bubbles, for j_l = 21.64 $\times 10^{-2}$ m/s and: a) j_g = 0.0 m/s; b) j_g = 2.38 $\times 10^{-3}$ m/s and α_g = 0.7 %; c) j_g = 19.83 $\times 10^{-3}$ m/s and α_g = 4.9 %.

5. CONCLUSIONS

The PIV/LIF measurement technique is often used in liquid-gas two-phase flows, but due to the presence of the gas phase, its application is restricted to flows with low gas fraction values or with large-scale gas-liquid interfaces, e.g., stratified or Taylor flows. In the literature, some studies seek to study detailed the flow around a Taylor bubble through the PIV/LIF technique (Van Hout *et al.*, 2002; Nogueira *et al.*, 2003, 2006; Meneghini, 2014), but none of the works describe the generation of masks to remove the Taylor bubble from the liquid phase velocity fields in the presence of dispersed bubbles. This work describes a method of generating dynamic masks for identification and removal of bubbles from Taylor in the application of the PIV/LIF technique. The method is used to study the flow around a bubble of Taylor ascending in a vertical flow with a column of liquid stagnated and in situation of flow "quasi-slug" (Meneghini, 2014). According to the results, the method successfully identifies the Taylor bubbles in the raw PIV images and removes its associates liquid velocity vectors from the instantaneous PIV fields. Through the obtained results, it is observed that the interaction between the dispersed and Taylor bubbles causes changes the liquid ensemble average velocity fields in the wake and nose region. Additionally, the image processing described in this work can be further extended to analyze real gas-liquid vertical and horizontal flows, providing new physical insights about heat and mass transfer process in those sort of flows.

6. ACKNOWLEDGEMENTS

This work was realized with the financial support of PETROBRAS, through the Human Resources Program PFRH.

7. REFERENCES

Bradski, G., 2000. "The opencv library." *Dr. Dobb's Journal: Software Tools for the Professional Programmer*, Vol. 25, No. 11, pp. 120–123.

Bugg, J.D. and Saad, G.A., 2002. "The velocity field around a Taylor bubble rising in a stagnant viscous fluid: Numerical and experimental results". *International Journal of Multiphase Flow*, Vol. 28, No. 5, pp. 791–803. ISSN 03019322. doi:10.1016/S0301-9322(02)00002-2.

Cerqueira, R., Paladino, E., Ynumaru, B. and Maliska, C., 2018. "Image processing techniques for the measurement of two-phase bubbly pipe flows using particle image and tracking velocimetry (piv/ptv)". *Chemical Engineering Science*.

Meneghini, C., 2014. *Caracterização Experimental Do Escoamento em Padrão Slug em Dutos Verticais com e sem Bolhas Dispersas*. Master's thesis, Universidade Federal de Santa Catarina.

Nogueira, S., Riethmuller, M.L., Campos, J.B. and Pinto, A.M., 2006. "Flow patterns in the wake of a Taylor bubble rising through vertical columns of stagnant and flowing Newtonian liquids: An experimental study". *Chemical Engineering Science*, Vol. 61, No. 22, pp. 7199–7212. ISSN 00092509. doi:10.1016/j.ces.2006.08.002.

Nogueira, S., Sousa, R.G., Pinto, A.M., Riethmuller, M.L. and Campos, J.B., 2003. "Simultaneous PIV and pulsed shadow technique in slug flow: A solution for optical problems". *Experiments in Fluids*, Vol. 35, No. 6, pp. 598–609. ISSN 07234864. doi:10.1007/s00348-003-0708-8.

Raffel, M., Willert, C.E., Wereley, S.T. and Kompenhans, J., 2007. *Particle Image Velocimetry*, Vol. 79. ISBN 9783540723073. doi:10.1007/978-3-540-72308-0.

Santos, L.M.T. and Coelho Pinheiro, M.N., 2014. "Flow around individual Taylor bubbles rising in a vertical column with water: Effect of gas expansion". *International Journal of Multiphase Flow*, Vol. 63, pp. 39–51. ISSN 03019322. doi:10.1016/j.ijmultiphaseflow.2014.03.003.

Sousa, R.G., Pinto, A.M.F.R. and Campos, J.B.L.M., 2006a. "Effect of gas expansion on the velocity of a Taylor bubble: PIV measurements". *International Journal of Multiphase Flow*, Vol. 32, No. 10-11, pp. 1182–1190. ISSN 03019322. doi:10.1016/j.ijmultiphaseflow.2006.06.002.

Sousa, R.G., Riethmuller, M.L., Pinto, A.M. and Campos, J.B., 2006b. "Flow around individual Taylor bubbles rising in stagnant polyacrylamide (PAA) solutions". *Journal of Non-Newtonian Fluid Mechanics*, Vol. 135, No. 1, pp. 16–31. ISSN 03770257. doi:10.1016/j.jnnfm.2005.12.007.

Sousa, R., Riethmuller, M., Pinto, A. and Campos, J., 2005. "Flow around individual Taylor bubbles rising in stagnant CMC solutions: PIV measurements". *Chemical Engineering Science*, Vol. 60, No. 7, pp. 1859–1873. ISSN 00092509. doi:10.1016/j.ces.2004.11.035.

Van Hout, R., Gulitski, A., Barnea, D. and Shemer, L., 2002. "Experimental investigation of the velocity field induced by a Taylor bubble rising in stagnant water". *International Journal of Multiphase Flow*, Vol. 28, No. 4, pp. 579–596. ISSN 03019322. doi:10.1016/S0301-9322(01)00082-9.

8. RESPONSIBILITY NOTICE

The authors are the only responsible for the printed material included in this paper.